This article was published in Water Research, 65 (15), 307-320, 2014
http://dx.doi.org/10.1016/j.watres.2014.07.037

Solar photocatalytic oxidation of recalcitrant natural metabolic by-products of amoxicillin biodegradation

João H.O.S. Pereira [a,1], Ana C. Reis [b,1], Vera Homem [b], José A. Silva [b], Arminda Alves [b], Maria T. Borges [c], Rui A.R. Boaventura [a], Vítor J.P. Vilar [a,*], Olga C. Nunes [b,**]

[a] LSRE - Laboratory of Separation and Reaction Engineering, Associate Laboratory LSRE/LCM, Faculdade de Engenharia, Universidade do Porto, Rua Dr. Roberto Frias, 4200-465 Porto, Portugal

[b] LEPABE - Laboratory of Process Engineering, Environment, Biotechnology and Energy, Faculdade de Engenharia da Universidade do Porto, Rua Dr. Roberto Frias, 4200-465 Porto, Portugal

[c] CIMAR - Centre for Marine and Environmental Research, Universidade do Porto and Departamento de Biologia, Faculdade de Ciências da, Universidade do Porto, Rua Campo Alegre, 4169-007 Porto, Portugal

Abstract

The contamination of the aquatic environment by non-metabolized and metabolized antibiotic residues has brought the necessity of alternative treatment steps to current water decontamination technologies. This work assessed the feasibility of using a multi-stage treatment system for amoxicillin (AMX) spiked solutions combining: i) a biological treatment process using an enriched culture to metabolize AMX, with ii) a solar photo-catalytic system to achieve the removal of the metabolized transformation products (TPs) identified via LC-MS, recalcitrant to further biological degradation. Firstly, a mixed culture (MC) was obtained through the enrichment of an activated sludge sample collected in an urban wastewater treatment plant (WWTP). Secondly, different aqueous matrices spiked with AMX were treated with the MC and the metabolic transformation products were identified. Thirdly, the efficiency of two solar assisted photocatalytic processes (TiO_2/UV or Fe^{3+}/Oxalate/H_2O_2/UV-Vis) was assessed in the degradation of the obtained TPs using a lab-scale prototype photoreactor equipped with a compound parabolic collector (CPC). Highest AMX specific biodegradation rates were obtained in buffer and urban wastewater (WW) media (0.10 ± 0.01 and 0.13 ± 0.07 gAMX $g_{biomass}^{-1} h^{-1}$, respectively). The resulting TPs, which no longer presented antibacterial activity, were identified as amoxicilloic acid (m/z = 384). The performance of the Fe /Oxalate/H_2O_2/UV-Vis system in the

removal of the TPs from WW medium was superior to the TiO2/UV process (TPs no longer detected after 40 min (QUV = 2.6 kJ L^{-1}), against incomplete TPs removal after 240 min (QUV = 14.9 kJ L^{-1}), respectively).

1. Introduction

In the last decades, the use of antibiotics has evolved from preventing and treating human and veterinary infections to other applications in diverse areas, such as agriculture, aquaculture and animal husbandry (Martinez, 2009). To this date, β-lactams remain one of the most important and pre- scribed group of antibiotics (Sun et al., 2012; Versporten et al., 2011), with amoxicillin (AMX), a broad-spectrum and semi- synthetic penicillin, as one of most relevant of its class. AMX is poorly metabolized in the organism and, consequently, around 80-90% is excreted in its original form (Hirsch et al., 1999). Despite the high consumption, AMX is infrequently detected in environmental samples. Raw wastewater con- centrations can vary from 0.02 to 6.9 μg L^{-1} and are easily eliminated by conventional treatments (Michael et al., 2013). The infrequent detection of AMX in the environment may be explained by low efficiency and sensitivity of extraction and detection methods, combined with the highly reactive β-lactam ring, which is broken under environmental conditions, such as alkaline conditions (pH 7.5e9.0), water hardness and by b-lactamase action (Babington et al., 2012; Deshpande et al., 2004; Hirsch et al., 1999; Jerzsele and Nagy, 2009). Nevertheless, the low persistence of AMX in water matrices may be compensated by its intensive use and continuous discharge into the environment (Daughton and Ternes, 1999).

Amoxicillin has low toxicity and, for that reason, direct effects in the environment are highly unlikely (Andreozzi et al., 2004). Nevertheless, indirect effects, such as propagation of β-lactam resistant bacteria (Martinez, 2009) and the impact of metabolites are more pressing concerns. Several studies reported an increasing proportion of b-lactam resistant organisms after wastewater treatment, which suggests that conventional WWTP may promote the spread of antibiotic resistance (Rizzo et al., 2013; Zhang et al., 2009). This could also explain the frequent presence of resistance genes in different environmental compartments such as surface and drinking water, a tendency reported for all the major antibiotic classes, including penicillins (Vaz-Moreira et al., 2014). Resistance against AMX and other penicillins can occur by different mechanisms, and deactivation of this group of antibiotics through the action of b-lactamases is one of the most common and relevant (Drawz and Bonomo, 2010). The products of AMX chemical or β-lactamase hydrolysis are, to some extent, more recalcitrant than the parent compound and for that reason, have

been frequently detected in both environ- mental samples and animal tissue (Lamm et al., 2009; Pérez- Parada et al., 2011; Reyns et al., 2008). Amoxicilloic acid is one of the major metabolites and in addition to its recalcitrant behaviour, this compound retains allergenic properties that can cause adverse reactions in sensitive individuals (Torres et al., 2010).

Given the aforementioned detrimental effects, the development of treatment methods able to remove antibiotic residues and their by-products is henceforth an environmental priority. Advanced oxidation processes (AOPs) are known as highly efficient methods to treat otherwise recalcitrant organic pollutants. They are characterized by different ways of generating the highly reactive and non-selective hydroxyl radical (•OH) and other reactive oxygen species (Gogate and Pandit, 2004a, b). As a way of reducing operating costs, recent research has been focussing on the combination of AOPs able to use solar radiation as the source of UV photons, such as TiO2/UV and the photo-Fenton process, with biological degradation as a pre- or post-treatment stage (Elmolla and Chaudhuri, 2011; González et al., 2008; Oller et al., 2011). Our research groups have previously dealt with each of these processes separately. Barreiros et al. (2003) and Lopes et al. (2013) successfully isolated bacteria commonly found in contaminated sites and applied them, *in situ*, for the biodegradation of an organic pollutant. Additionally, Pereira et al. (2013a, 2013b); Pereira et al. (2014) reported on the removal of antibiotics such as Amoxicillin, Oxytetracycline and Oxolinic Acid from aqueous solutions by solar TiO2-assisted photocatalysis and by the ferrioxalate-mediated solar photo- Fenton process using a pilot-plant equipped with compound parabolic collectors (CPCs). Although Amoxicillin has been previously subject to several degradation studies via various AOPs (Ay and Kargi, 2011; Dimitrakopoulou et al., 2012; Homem et al., 2010; Mavronikola et al., 2009; Trovó et al., 2011), none has focused on the removal of common transformation products resulting from the slow transformation that the parent compound undergoes in aquatic environ- ments (Gozlan et al., 2013; Längin et al., 2009; Nägele and Moritz, 2005). In this way, the aim of this study was to evaluate a multistage treatment for AMX-spiked solutions combining: i) a biological treatment step to metabolize the AMX molecule, with ii) a solar photocatalytic system to achieve the mineralization of the transformation products (TPs), recalcitrant to further biological removal. Firstly, a mixed culture (MC) was obtained through the enrichment of an activated sludge sample collected in a WWTP treating urban wastewater in order to optimize AMX biotransformation. Secondly, different aqueous matrices spiked with AMX were treated with the MC, which constituted a surrogate of activated sludge, and the metabolic transformation products were identified. Thirdly, the efficiency of the

photocatalytic step was assessed in the removal of the metabolized TPs in a lab-scale photoreactor prototype equipped with a compound parabolic collector (CPC). The two proposed solar AOPs are the well-known photocatalytic system mediated by TiO_2 (TiO_2/ UV) and a modification of the conventional photo-Fenton process in order to work with near-neutral pH levels, the Fe^{3+}/Oxalate/H_2O_2/UV-Vis system. To the best of the authors' knowledge, this is the first study dealing exclusively with the application of AOPs to remove recalcitrant transformation products resulting from the natural degradation of antibiotics, which are often overlooked.

2. Materials and methods

2.1. *Reagents*

Amoxicillin (MW: 365.4, CAS# 26787-78-0, HPLC-UV chromatogram and MS/MS spectrum in Fig. 1a and b, respectively) was purchased from Sigma-Aldrich. HPLC-grade methanol was from Prolabo, H_3PO_4 (85% p.a.), KH_2PO_4 and $(NH_4)_2SO_4$ from Merck (analytical grade) and yeast extract (YE) from Fisher Scientific. For the LC-MS analysis, methanol hyper- grade for LC-MS (LiChrosolv®) from Merck, water LC-MS Chromasolv® and formic acid (98% p.a.) from Fluka were used. Syringe filters with 0.2 mm nylon membranes were purchased from Whatman and 0.45 mm nylon filter mem- branes from Supelco. Titanium dioxide used in photocatalytic experiments was Degussa P25 (80% anatase and 20% rutile). Photo-Fenton experiments were performed using hydrogen peroxide (Quimitécnica, S.A., 50% (w/v), 1.10 g cm^{-3}), iron (III) chloride hexahydrate (Merck) and oxalic acid dihydrate (VWR Prolabo, purity 98%). Sulfuric acid (Pronalab, 96%, 1.84 g cm^{-3}) and sodium hydroxide (Merck) were used for pH adjustment.

2.2. *Microbial culture media*

Mineral medium B (Barreiros et al., 2003) was used as microbial growth medium, supplemented with 0.53 g L^{-1} $(NH_4)_2SO_4$ and 1 g L^{-1} yeast extract (YE) as nitrogen and carbon sources, respectively. This medium (pH = 7.2), hereafter designated as enrichment medium (EM), was supplemented with 0.01-0.03 g L^{-1} of AMX. Antibiotic stock solutions were prepared weekly in distilled water at a final concentration of 2 g L^{-1} and kept at −20 °C prior to use.

2.3. *Obtainment of a microbial culture enriched in AMX degraders*

A sample from the aerobic activated sludge biological reactor collected in an urban WWTP (Northern Portugal) was diluted 2-fold in EM initially spiked with 0.01 g L^{-1} AMX. The enrichment culture was successively transferred to fresh medium with increasing AMX content, up to 0.03 g L^{-1}, and with initial cell densities corresponding to 0.02 g L^{-1} dry weight. Transferences were performed for 24 weeks at intervals of 1∈15 d. Cultures were incubated at 30 °C and 120 rpm. The final culture obtained, which was used as a surrogate of activated sludge in the combined treatment system, was named mixed culture (MC).

2.4. *Bacteria isolation, characterization and identification*

The MC was serially diluted in sterile saline solution (0.85%, w/ v), spread on Plate Count Agar (PCA) supplemented with AMX (0.03 g L^{-1}) and incubated at 30 °C for 48 h. Individual colonies with distinct morphologies were purified by subculturing on the same medium. Isolates were identified by 16S rRNA gene sequence analysis. Amplification of the gene was performed by PCR using universal primers 27F (5'-AGAGTTT- GATCMTGGCTCAG-3') and 1492R (5'-TACCTTGTTACGACTT-3') (Lane, 1991). Nucleotide sequences were compared to those available in public databases using Eztaxon server (http:// www.ezbiocloud.net/eztaxon) (Kim et al., 2012).

Resting cells assays, performed according to Barreiros et al. (2003), were carried out with each distinct isolate to determine their role in AMX degradation.

2.5. *Combined treatment process*

In order to assess the influence of the aqueous matrix composition on the efficiency of the treatment, assays were carried out in EM, saline solution (NaCl, 0.85%, w/v), phosphate buffer (Buffer; 50 mM, pH 7.2), and wastewater (WW) collected after secondary wastewater treatment in an urban WWTP (in Northern Portugal). The main characteristics of each medium are presented in Table 1. The high initial AMX concentration, 0.02 g L^{-1}, was chosen to properly follow the formation and depletion of the TPs by HPLC-UV/Vis analysis.

2.5.1. *Biological treatment*

The biological treatment step was carried out in a batch sys- tem using a 5 L

Erlenmeyer flask, containing 1.2 L of the test matrix spiked with 0.02 g L^{-1} of AMX, in parallel with a control flask to monitor abiotic degradation.

Inoculum was previously obtained by growing the MC in EM spiked with 0.02 g L^{-1} AMX. Cells were harvested at the late exponential phase, washed twice and resuspended in sterile saline solution (0.85%, w/v). Given the inability of cells to grow in the absence of macro- and micronutrients, decreasing complexity of the tested matrices demanded increasing initial biomass concentration. For the experiments carried out in EM, 0.03 g L^{-1} of cell dry weight was used, in phosphate buffer, 0.11 g L^{-1}, and for both saline solution and real wastewater, 0.26 g L^{-1}. MC cells were separated from the respective medium by centrifugation at 26,000 × *g* when AMX was found in residual concentrations (0.57-1.97 g L^{-1}). As expected due to the low organic carbon content (DOC ranging between 10 and 25 mg L^{-1} after spiking with AMX and MC inoculation), for the experiments in Buffer, NaCl and WW matrices, no bacterial growth was observed, and AMX degradation followed zero order kinetics. The degradation rate was obtained by simple linear regression, as expressed by Eq. (1):

$$S = S_0 - kt \quad (1)$$

where S represents the substrate content at time t (mg L^{-1}), S_0 the substrate content at t = 0, t the time (h) and k the degradation rate (h^{-1}). The half-life ($t_{1/2}$) and the specific degradation rates (k_S) were calculated as follows (Eqs. (2) and (3)):

$$t_{1/2} = \frac{S_0}{2k} \quad (2)$$

$$k_s = \frac{k}{X} \quad (3)$$

where X represents the biomass content in cell dry weight (mg L^{-1}).

2.5.2. *Solar photocatalytic treatment*

In all experiments, 1.1 L (Vt) of the resulting supernatant from the biological treatment step was transferred into the recirculation glass vessel of the lab-scale photoreactor provided with a sunlight simulator (SUNTEST). A schematic

representation and a detailed description can be consulted elsewhere (Soares et al., 2014). Two AOPs, the TiO_2/UV system or the Fe^{3+}/Oxalate/H_2O_2/UV-Vis process, were performed in order to assess their efficiency in the degradation and mineralization of the AMX metabolic by-products. The pH was not controlled in any of the reactions, in both AOP systems.

In the TiO_2/UV experiments, 0.2 g L^{-1} of TiO_2 was added to the bio-treated wastewater, the pH was adjusted to 5.5 with sulfuric acid and the solution was left to homogenize in darkness for 30 min. This TiO_2 concentration was chosen because it is considered to be the optimal concentration when working with the CPC unit described in this work (internal diameter 46.4 mm) (Rodríguez et al., 2004), and is estimated to be able to absorb 100% of the incoming solar UV photons (Colina-Márquez et al., 2010). Before irradiation began, a sample was taken to check initial AMX and DOC concentration and TPs' HPLC-UV areas.

In the Fe^{3+}/Oxalate/H_2O_2/UV-Vis experiments, oxalate was first added to the supernatant in a 1:3 (NaCl matrix) or 1:9 (WW matrix) iron/oxalate molar ratio dose and a sample was taken after 15 min. The pH was adjusted to 4.0 or 5.0 and iron (III) chloride was then added to achieve a concentration of 2 mg L^{-1} Fe (III), the total iron discharge limit into any water body, according to Portuguese legislation (Decree-Law n.º 236/ 1998). Any marginal effect on pH was then corrected, and the solution was left to homogenize for 15 min. Another sample was then taken, and the initial iron concentration was also confirmed. The solution was then pumped to the CPC unit (illuminated volume (V_i) = 270 mL; V_i/V_t ~ 0.24; A_{CPC} = 0.025 m^2) before the SUNTEST was turned on. Irradiation was set as I = 500 WUV m^{-2}, which is equivalent to 44 WUV m^{-2} measured in the wavelength range from 280 to 400 nm. Immediately after irradiation began, the initial H_2O_2 dose was added, while the pH of the solution was left uncontrolled. To avoid excess H_2O_2 in solution, a controlled dosage strategy was followed as suggested by Klamerth et al. (2010), starting with an initial 30 mg L^{-1} (~0.9 mM) dose at the beginning of every experiment, with supplementary 30 mg L^{-1} additions performed along the reaction whenever the H_2O_2 concentration in solution approached 10 mg L^{-1}.

Samples were taken during the experiments at pre-defined times and filtered through 0.45 mm Nylon VWR membrane filters before analysis to evaluate the photodegradation process. For HPLC analysis, samples were quenched with methanol to stop any further reactions, while DOC analysis was performed immediately, without pretreatment.

2.6. Analytical procedures

AMX concentration and transformation products (TPs) areas were obtained by HPLC, in a system equipped with an UV⊖Vis detector (Knauer), operating at 230 nm and using a 5 mm Superspher 100 RP-18e (125 x 4 mm) column from Merck. For the mobile phase, a mixture of 96% (v/v) KH_2PO_4 buffer (50 mM) and methanol acidified at pH 3 with ortophosphoric acid was used at 1 mL min^{-1}. Retention time for AMX was 11.8 ± 0.2 min. TP1, TP2, TP3 and TP4 were detected at 8.3 ± 0.2, 6.80 ± 0.09, 4.10 ± 0.03 and 2.70 ± 0.01 min, respectively.

Identification of the TPs was performed using a Varian LC- MS system (Lake Forest, USA), constituted by a ProStar 210 Binary Solvent Delivery Module and a 500-MS LC Ion Trap Mass Spectrometer, equipped with an electrospray ionization source (ESI). Data was acquired and processed by Varian MS Workstation Version 6.9 software. A Pursuit® XRs Ultra C18 column (100 mm x 2.0 mm i.d., particle size: 2.8 μm), in combination with a MetaGuard column Pursuit® C18 (10 mm x 2.0 mm i.d., particle size: 5 μm) were purchased from Varian (Lake Forest, USA). The mobile phase was composed of 96% water with 0.1% formic acid and 4% methanol, running in isocratic mode at a flow rate of 0.2 mL min^{-1}. The injection volume was 10 mL. The mass spectrometer had an electrospray interface operated in positive mode using: capillary voltage, 69.0 V; shield voltage, 600 V; needle voltage, 3453 V; RF loading, 90%; drying gas pressure, 15 psi; drying gas temperature, 250 °C; nebulizing gas pressure, 50 psi; multiplier offset, 300 V; MS scan range, 50-600 m/z.

Cell growth was measured by optical density (OD610) using a UV/Vis Unicam Helios spectrophotometer and by dry weight using a calibration curve. The later was obtained by filtering cell suspensions through 0.45 mm membranes (Advantec), dried at 70 °C until constant weight.

Growth inhibition assays were carried out in 96-well microtiter plates using a Synergy HT Multi-Mode Microplate Reader (Biotek Instruments, USA) in order to test the toxicity of treated samples. *Escherichia coli* (DSM 1103) and *Staphylococcus aureus* (DSM 1104) were used as test strains. Minimum inhibitory concentration (MIC) for each strain is 4.0 and 0.25 mg AMX L^{-1}, respectively (Andrews, 2001). Each plate, in addition to the treated samples, contained both negative and positive controls (inoculated media with and without 0.02 g L^{-1} AMX, respectively), and blanks (cell-free media). All wells were supplemented with 2 g L^{-1} YE and the plates were then incubated at 30 °C, continuously shaken for 20 h, with absorbance measurements at 610 nm every 30 min. Each sample was tested in triplicate and a first-order kinetic model was

used to fit the experimental data, being the specific growth rate (h^{-1}) normalized by that of the positive control. Comparison of means was made by a one-way ANOVA test using *R* software (R Development Core Team, 2013).

Concentration of H_2O_2 was measured by the metavanadate method, according to Nogueira et al. (2005). Dissolved iron concentration was determined by colourimetry with 1,10- phenantroline, according to ISO 6332.

A detailed description of the analysis of dissolved organic carbon (DOC) content (TC-TOC-TN analyzer), and low- molecular-weight carboxylate anions (LMWCA, ion chromatography) can be consulted elsewhere (Pereira et al., 2013b). Additional LMWCA analysis was performed in the HPLC-DAD system, using a Rezex™ ROA-Organic Acid H^+ (8%), LC Column 300 x 7.8 mm. The isocratic method used 0.005 N H_2SO_4 delivered at a flow rate of 0.5 mL min^{-1}. Run time was 50 min, injection volume 10 µL and the wavelength of the detector was set at 210 nm. Sulfate, chloride and phosphate were quantified by ion chromatography (Dionex ICS-2100; column AS 11-HC 4 x 250 mm; suppressor ASRS 300 4 mm). Isocratic elution was performed using 30 mM NaOH at a flow rate of 1.5 mL min^{-1}.

Eq. (4) allows the calculation of the accumulated UV energy ($Q_{UV,n}$ kJ L^{-1}) received on any surface in the same position with regard to the lamp, per unit of volume of water inside the reactor, in the time interval Δt:

$$Q_{UV,n} = Q_{UV,n-1} + \Delta t_n \overline{UV}_{G,n} \frac{A_r}{1000 \times V_t}; \quad \Delta t_n = t_n - t_{n-1} \qquad (4)$$

where t_n is the experimental time of each sample (s), V_t the total reactor volume (L), A_r the illuminated collector surface area (m^2) and $\overline{UV}_{G;n}$ the average solar ultraviolet radiation (W m^{-2}) measured during the period Δt_n (s).

3. Results and discussion

3.1. *Characterization of the mixed culture (MC)*

A mixed culture (MC) able to degrade AMX was obtained after enrichment of activated sludge with this antibiotic. MC was able to grow unimpaired up to 0.45 g L^{-1} AMX in the presence of 1 g L^{-1} YE. However, no growth was observed when AMX acted as a sole carbon source (data not shown). The spread plate method revealed the presence of 33 different morphotypes, which were affiliated

to 6 distinct genera (Table 2).

All organisms were Gram-negative and the majority was affiliated to the phylum *Proteobacteria*, known to be common inhabitants of activated sludge (Zhang et al., 2012). Within this group a high percentage of isolates was closely related to *Citrobacter freundii*, followed by *Stenotrophomonas acid- aminiphila*. Although in lower proportion, members of the phylum *Bacteroidetes* were also isolated. When individually tested in phosphate buffer (0.05 M, pH 7.2, 0.035 g L^{-1} AMX), resting cells of all isolates were able to degrade AMX, albeit at different rates. The overall specific degradation rate of the MC (0.11 g_{AMX} $g_{biomass}^{-1}h^{-1}$) closely corresponded to that of *C. freundii* (0.09 g_{AMX} $g_{biomass}^{-1}h^{-1}$). Other isolates exhibited either slower (*Elizabethkingia meningoseptica*, 0.03 g_{AMX} g $g_{biomass}^{-1}h^{-1}$), or higher (*Stenotrophomonas nitritireducens*, 2.95 g_{AMX} $g_{biomass}^{-1}$ h^{-1}) degradation rates.

These results suggest that all the isolates express β-lactamases. Indeed, members of the same taxa have been described as carriers of different b-lactam resistance genes (Gonzalez and Vila, 2012; Henriques et al., 2012; Literacka et al., 2004; Vaz-Moreira et al., 2011). In addition, AmpC β- lactamase, a class C serine cephalosporinase, is frequently found in enterobacteria, such as *C. freundii* (Drawz and Bonomo, 2010), while metallo- β-lactamases, class B zinc β-lactamases, are expressed by members of *E. meningoseptica*, *Stenotrophomonas* sp. and *Pseudomonas* sp. (Drawz and Bonomo, 2010; Galleni et al., 2001), which are able to degrade most β-lactam antibiotics including carbapenems (Walsh et al., 2005). Given their wide diversity (Drawz and Bonomo, 2010), β-lactamases may possess different affinities for AMX, which may explain the significant differences in the degradation rates observed in the present study. Because a mixed culture is a better surrogate of activated sludge than axenic bacterial cultures, MC was further used in the combined treatment.

3.2. *Combined treatment for AMX removal*

In order to assess the influence of the aqueous matrix composition in the efficiency of the combined treatment, as- says were performed in EM, Buffer and NaCl solution. Given our major aim was the assessment of the feasibility of using this process in the decontamination of real waters, the efficiency of the combined system in the removal of AMX and degradation products thereof was also carried out in treated urban wastewater.

3.2.1. *Biological degradation step performance*

In all tested matrices, the biodegradation of AMX occurred concomitantly with

the accumulation of TP1, which subsequently yielded TP2, both detected by HPLC analysis (HPLC- UV/Vis chromatograms in Fig. 1a). Further analysis of these metabolites by LC-MS/MS indicated that they had similar mass spectra, equivalent to that of amoxicilloic acid ($[C_{16}H_{21}N_3O_6S + H]^+$, m/z = 384, Fig. 1c), the product of b- lactamase action (Deshpande et al., 2004; Nägele and Moritz, 2005). Although LC-MS/MS was unable to distinguish TP1 from TP2, these products were, probably, the stereoisomers (5*R*,6*R*) and (5*S*,6*R*) of amoxicilloic acid, identified before (Pérez-Parada et al., 2011). The results obtained in the present study suggest that the enzymatic catalysis favours the formation of one of the isomers. This behaviour was also observed by Lewis et al. (1997), which confirmed the formation of the (5*R*,6*R*) isomer mediated by a serine β-lactamase and consequent epimerization to the (5*S*,6*R*) configuration by non-enzymatic mechanisms. The hydrolysis of the b-lactam ring results in the total loss of antimicrobial activity, which was herein confirmed by experimental data. By the end of the biological step, the liquid phase no longer inhibited the growth of *E. coli*, whereas its effect against *S. aureus* was greatly reduced, as shown, as an example, in the experiment performed in the NaCl matrix (Fig. 2).

AMX hydrolysis by the MC followed a zero-order kinetic model, except in the assay carried out in EM. In this particular case, the presence of YE resulted in increasing biomass con- tent over time, with the degradation following first-order kinetics, not allowing a direct comparison with the experiments carried out in other matrices. AMX biodegradation was significantly faster ($p < 0.05$) in Buffer and WW than in the NaCl matrix, while Buffer and WW matrices displayed similar specific degradation rates ($p > 0.05$) (Table 3).

These differences can be explained by the distinct chemical composition and pH values of each matrix. The comparatively higher ionic strength, lower pH and lack of buffer capacity of the NaCl matrix have probably contributed for these results. Indeed, NaCl is a weak inhibitor of OXA-type β- lactamases (Afzal-Shah et al., 2001). The high standard deviation observed for the WW experiments may be explained by variations in its chemical and microbiological composition. Abiotic degradation of the parent compound in the cell-free matrix was negligible for all experiments (data not shown).

TP1/TP2 exhibited a recalcitrant behaviour, since the MC could not remove them even after 46 d of incubation (data not shown). This observation is supported by Gozlan et al. (2013) who detected amoxicilloic acid at relatively high concentrations (mg L^{-1}) in secondary effluents used for irrigation, as well in the underground water collected in a well located in the irrigated field.

Given that TP1/2 result from the hydrolysis of the beta- lactam ring, the DOC remained constant in all experiments, except in the EM matrix, where the

consumption of YE by the MC led to a 25% decrease in the initial carbon content (Fig. 3a and b, left side). These results and observations highlight the need of complementing AMX biodegradation with the proposed photocatalytic methods for the removal and mineralization of the resulting transformation products.

For the combined treatment assays, the endpoint of the biological step was set between 90 and 95% of AMX depletion, which corresponded to incubation periods ranging from 3.2 to

4.8 h, for Buffer and NaCl matrices, respectively (Table 3). However, possibly given the high stability of the b-lactamases produced by the MC members and extracellular release by leakage into the medium (Livermore, 1995), AMX transformation was not hampered during the processing of the samples, and transference of the supernatant into the photoreactor. Consequently, the AMX concentration at the beginning of the AOPs treatments was below the quantification limit (0.5 mg L^{-1}) (Fig. 4a and b, before irradiation). As expected, by the end of the biological degradation step, no significant DOC reduction was observed in all the matrices with low initial DOC content (0 to approximately 1 mg L^{-1} of DOC reduction). In opposition, the utilization of yeast extract as carbon and energy source allowed a DOC reduction of about 25% in the EM matrix.

3.2.2. *TiO2/UV photocatalysis step performance*

During preliminary TiO_2/UV photocatalytic experiments, where the pH was kept unchanged, the removal of TP1/TP2 was remarkably slow (data not shown), with no apparent mineralization. To the best of our knowledge, no information regarding the pK_a constants of TP1/TP2 is available, thus not allowing any direct conclusion regarding the role of electro- static attraction between TiO_2 particles and TP1/TP2 molecules. For that reason, all the matrices were acidified (5.5) prior to photocatalytic treatment to take advantage of the positive effect of increased catalyst surface when smaller TiO_2 particle size is favoured under pH values lower than the Point of Zero Charge of Degussa P25 (pH_{PZC} = 6.7 (Malato et al., 2009)), as recommended by Li et al. (2010).

The NaCl solution was the most favourable matrix, as TP1 and TP2 were no longer detected after 90 min of illumination (Q_{UV} = 5.3 kJ L^{-1}), followed by the Buffer matrix, which required 180 min of illumination (Q_{UV} = 10.9 kJ L^{-1}). However, a third unidentified TP (TP3) accumulated in all matrices (Fig. 3a and b). In the WW experiment, a fourth product also accumulated (TP4), albeit transiently (Fig. 3b).

Differences in matrices complexity in EM and WW experiments seem to account for the inability of completely removing TP1/TP2 under similar photo-treatment periods. The pronounced amount of organic matter compared to the simpler matrices may have not only competed with the catalyst for absorption of incident UV radiation, but also with the TP1/TP2 attack by the generated •OH radicals. Controls were performed in the absence of light and no considerable effects were found. Despite the initial decreases in the DOC content due to the adsorption of organic matter onto the surface of the catalyst, no notable DOC removal occurred during the illumination period. This can be explained by the high concentrations of Cl^- (NaCl) and $PO4^{3-}$ (Buffer) in the respective matrices, which might have affected the mineralization process via competitive adsorption onto the TiO_2 sur- face, their •OH radical scavenger properties, and finally, via the formation of less reactive inorganic radicals, as suggested by Guillard et al. (2005) and De Laat et al. (2004). The exception was the NaCl experiment, which saw a 35% DOC reduction after 180 min, when compared to the initial value before the catalyst addition step (Fig. 3b).

3.2.3. *Photo-Fenton step performance*

Given the apparent unsuitability of using the TiO_2/UV system with the most realistic matrix (WW), the Fe^{3+}/Oxalate/H_2O_2/ UV-Vis system was tested as an alternative suited to near- neutral pH levels. Beforehand, some considerations about this treatment must be made. The conventional photo-Fenton process, as simplified by Gogate and Pandit (2004b), comprises the combination of ferrous iron (Fe^{2+}) with hydrogen peroxide (H_2O_2) and (solar) UV-Vis radiation resulting in the production of two moles of •OH per mole of hydrogen peroxide (Eqs. (5) and (6)):

$$Fe^{2+} + H_2O_2 \rightarrow Fe^{3+} + \cdot OH + HO^- \quad (5)$$

$$Fe(OH)^{2+} + h\upsilon \rightarrow Fe^{2+} + \cdot OH \quad (6)$$

The solubility of Fe^{3+}-hydroxy complexes, especially considering the molar fraction of the most photoactive species, $[Fe(OH)]^{2+}$ (with absorption bands between 290 and 400 nm), is very limited for pH values above 3 (Pignatello et al., 2006), which would demand additional costs of initial acidification and final neutralization of the solution. However, this can be overcome by means of the formation of Fe(III)- carboxylate complexes, which are able to extend the solubility of iron to near neutral pH working conditions. At the same time, these

complexes present stronger radiation absorption at wavelengths up to 580 nm and can increase the quantum yield of Fe^{2+} production according to Eq. (7) (Jeong and Yoon, 2005; Pignatello et al., 2006):

$$Fe^{3+}(C_2O_4)_n^{(3-2n)} + h\upsilon \rightarrow Fe^{2+} + (n-1)C_2O_4^{2-} + C_2O_4^{2-\bullet} \quad (7)$$

For this reason, the Fe(III)-oxalate complex was chosen, as the quantum yield of its two most photo-active species, $Fe(C2O4)_2^-$ and $Fe(C2O4)_3^{3-}$, were reported by Faust and Zepp (1993) as being 1.0 and 0.6 (436 nm), respectively. The working pH of the consequent experiments was decided according to the distribution of these species in solution. In view of that, MINEQL þ software was used to study the distribution of the Fe (III) complexes as a function of pH. The presence of inorganic ions such as $PO4^{3-}$, $SO4^{2-}$ and Cl^- in the different matrices (Table 1), which can compete with oxalate for available iron, thus hindering the process performance (De Laat et al., 2004), was also considered. The following oxalate and iron-oxalate equilibrium reactions were introduced in MINEQL+, with dissociation constants (Panias et al., 1996) corrected using the Davies equation for the approximate ionic strength of the corresponding matrix:

$$H_2C_2O_4 \leftrightarrow HC_2O_4^- + H^+ \quad (8)$$

$$HC_2O_4^- \leftrightarrow C_2O_4^{2-} + H^+ \quad (9)$$

$$Fe^{3+} + HC_2O_4^- \leftrightarrow FeHC_2O_4^{2+} \quad (10)$$

$$Fe^{3+} + C_2O_4^{2-} \leftrightarrow FeC_2O_4^+ \quad (11)$$

$$FeC_2O_4^+ + C_2O_4^{2-} \leftrightarrow Fe(C_2O_4)_2^- \quad (12)$$

$$Fe(C_2O_4)_2^- + C_2O_4^{2-} \leftrightarrow Fe(C_2O_4)_3^{3-} \quad (13)$$

Notwithstanding the use of the iron(III)-oxalate complexes, the solubility/concentration of iron (III) would be highly limited by the high phosphate content of the Buffer and EM media, which would result in the immediate precipitation of the mineral Strengite ($FePO4.2H2O$). Additionally, the amount of organic carbon of the EM matrix would also be highly deleterious. For these reasons, photo-Fenton experiments were not performed in these two

matrices.

Fig. 4 a and b shows the calculated iron speciation diagrams according to the molar concentration of each known component (Table 1) for NaCl and WW, respectively, in the absence (left) or in the presence (right) of oxalate. Initially, a 1:3 Fe(III)-oxalate molar ratio was considered to ensure the formation of the three photo-active complexes. The respective inorganic anion content of NaCl and WW was not expected to interfere in the formation of the Fe(III)-oxalate complexes. Despite this, WW experiments eventually required a higher iron/oxalate molar ratio dose (1:9), than NaCl matrix (1:3), resulting in remarkably different profiles.

In experiments performed with the initial 1:3 iron/oxalate molar ratio dose (data not shown), the added oxalate was not sufficient to keep a satisfactory Fe(III) concentration in solution along reaction time, due to the probable binding of iron to natural dissolved organic matter contained in the WW matrix (Lindsey and Tarr, 2000).

Ultimately, Fe^{3+}/Oxalate/H O /UV-Vis experiments were performed in NaCl and WW under two initial pH values, 4 and 5, as both $Fe(C_2O_4)_2^-$ and $Fe(C_2O_4)_3^{3-}$ are prominent in this pH range. Higher pH values were not considered due to the fact that in NaCl matrix the Ferrihydrite ($Fe(OH)_3$ (s)) fraction is shown to quickly rise near pH = 5.0, and becomes dominant at pH = 6.0 (Fig 4a), while in WW matrix, iron is expected to precipitate in the form of Strengite ($FePO_4.2H_2O$) after pH = 5.5, and as Ferrihydrite ($Fe(OH)_3$ (s)) after pH = 6.0 (Fig. 4b).

The results on TP1/TP2 removal from NaCl and WW matrix can be seen in Fig. 5a and b (right), respectively.

Compared to the TiO_2/UV system, TP1/TP2 removal was clearly improved, in both matrices and respective pH_0 values. In both pH_0 = 4.0 experiments, TP1/TP2 were no longer detected after 20 min of illumination (Q_{UV} = 1.3 kJ L^{-1}), while the pH_0 = 5.0 experiments required a longer period of illumination, 40 min (Q_{UV} = 2.6 kJ L^{-1}). In WW experiments, a third unidentified TP (TP3) appeared at 10 min of illumination, but it was no longer detected after 60 min (Q_{UV} = 4.0 kJ L^{-1}). Control experiments performed in darkness did not show significant TP1/TP2 removal in the same period. The general influence of pH on the experiments may be explained with the distribution of the above mentioned Fe (III)-oxalate species. Even considering the differences in their relative proportion over pH due to different iron/oxalate molar ratio doses, the fraction of most photo-active species, $Fe(C_2O_4)_2^-$, tends to be higher

around pH = 4.0, compared to pH = 5.0. The higher consumption of H_2O_2 seems to attest to this fact.

The process details for both matrices can be seen in Fig. 5a and b. By the end of the first 30 min of illumination (Q_{UV} = 1.9 kJ L^{-1}), an overall steady decrease can be seen in total soluble iron concentration. This corresponded well with the concomitant ongoing depletion of oxalate, apparent in HPLC analysis of low-molecular-weight carboxylate anions (LMWCA). With dwindling amounts of oxalate in solution, the distribution of iron (III) species seen in the right side of Fig. 4a and b would progress into what can be seen in the left side of the same Figure.

Up until this point in both NaCl matrix experiments, nevertheless, reduction of DOC exceeded the oxalate depletion, and an average of 45% of the remaining DOC was already in the form of tartronate, oxamate, malonate, glycolate, formate and acetate, besides a lower amount of oxalate itself.

In both WW experiments, on the other hand, DOC decreased along with the oxalate depletion, with vestigial amounts of other LMWCA.

Given the abovementioned fact that, in each matrix and tested pH_0 level, complete, or near complete TP1/TP2 removal occurred by 40 min of illumination, the process was extended with additional dosages of oxalate (marked as +Ox in Fig 6 a and b), in order to keep iron in solution and see the effects on the remaining DOC content.

Notwithstanding the added carbon with each oxalate addition, and the apparent levelling of DOC content in both NaCl and WW experiments, depletion of oxalate was quick between additions. After 120 min of illumination (Q_{UV} = 8.3 kJ L^{-1}) in NaCl experiments, an average of 55% of the final DOC content was in the form of LMWCA. In WW medium, only the pH_0 = 4.0 experiment benefited with the additional oxalate, as it can be seen in the progressive decrease of DOC content and its final 48% amount in the form of LMWCA, compared to 28% in the case of pH_0 = 5.0. In the same irradiation period, initial DOC concentration was altogether reduced in the NaCl matrix by 54% (pH_0 = 4.0) and 51% (pH_0 = 5.0), while in the WW matrix it was reduced by 48% (pH_0 = 4.0) and 21% (pH_0 = 5.0).

4. Conclusions

In this work, a mixed culture able to degrade the antibiotic Amoxicillin in different matrices was successfully obtained and characterized. AMX removal was concomitant with the accumulation of transformation products, which were

putatively identified as stereoisomers of amoxicilloic acid, and did not show antibacterial activity. However, they resisted further bacterial action, which brought up the need of a further, more efficient treatment. In this way, a complementary photo- catalytic oxidation step was proposed to enhance AMXC degradation in a lab-scale apparatus simulating solar radiation, equipped with a CPC photo-reactor. The first process proposed was a photocatalytic system promoted by 0.2 g L^{-1} of TiO_2 (TiO_2/UV), carried out at pH_0 = 5.5. In NaCl and Buffer, the respective TP1/TP2 peaks were no longer detected after 90 (Q_{UV} = 5.3 kJ L^{-1}) and 180 (Q_{UV} = 10.9 kJ L^{-1}) min of illumination. In the most complex matrices (EM and WW), however, TPs were still present after 180 min, the end of the irradiance period. Additionally, none of the TiO_2/UV experiments showed considerable DOC removal (maximum of 35% during the NaCl experiment). The second process proposed was the photo-Fenton reaction enhanced by the Fe(III)-oxalate complex (Fe^{3+}/Oxalate/H_2O_2/UV-Vis), carried out using 2 mg Fe(III) L^{-1}, a 1:3 (NaCl) or 1:9 (WW) iron/oxalate molar ratio and a total H_2O_2 addition of 90 mg L^{-1}. Based on the distribution of the two most photo-active species, $Fe(C_2O_4)_2^{-}$ and $Fe(C_2O_4)_3^{3-}$, experiments with NaCl and WW were performed under two initial pH values, 4.0 and 5.0. Substantially lower amounts of accumulated UV energy per litre TP1/TP2 of solution were required to remove TP1/TP2, compared to the TiO_2/UV ex- periments. With both pH_0 = 4.0 experiments, 20 min (Q_{UV} = 1.3 kJ L^{-1}) were necessary, while with pH_0 = 5.0 experiments, 40 min (Q_{UV} = 2.6 kJ L^{-1}) sufficed to remove TP1 and TP2. Regardless of the need of supplementary oxalate additions to extend the process beyond TP1/TP2 removal, the remaining carbon content was either converted to easily biodegradable low-molecular-weight carboxylate anions or removed in higher proportions after only 120 min (Q_{UV} = 8.3 kJ L^{-1}), the end of the photocatalytic step. The Fe^{3+}/ Oxalate/H_2O_2/UV-Vis system should thus be preferred for this kind of treatment, even at near neutral pH levels. Generally speaking, research concerning treatment methods to remove pharmaceuticals such as antibiotics from effluents mainly focuses on the parent compounds. Nevertheless, importance must also be given to naturally occurring by-products, which can also present environmental risks by themselves. In this way, combined treatments, such as the one proposed in this work, should be further developed for safe effluent discharge.

Acknowledgements

This work was co-financed by FCT and FEDER under Programe COMPETE (Projects PEst-C/EQB/LA0020/2013 and PTDC/AAC- AMB/113091/2009) as also by QREN, ON2 and FEDER through project NORTE-07-0162-FEDER-000050 and AQUAPHOTOBIO - PP-IJUP-2011-180 by University of Porto. J.H.O.S. Pereira and A.C. Reis acknowledge their doctoral fellowships (SFRH/BD/ 62277/2009 and SFRH/BD/95814/2013) supported by FCT. V. Homem acknowledges her post-doctoral fellowship (SFRH/ BDP/76974/2011) supported by FCT. V.J.P. Vilar acknowledges the FCT Investigator 2013 Programme (IF/01501/2013).

References

Afzal-Shah, M., Woodford, N., Livermore, D.M., 2001. Characterization of OXA-25, OXA-26, and OXA-27, molecular class D beta-lactamases associated with carbapenem resistance in clinical isolates of Acinetobacter baumannii. Antimicrob. Agents Chemother. 45 (2), 583-588.

Andreozzi, R., Caprio, V., Ciniglia, C., de Champdore', M., Lo Giudice, R., Marotta, R., Zuccato, E., 2004. Antibiotics in the environment: occurrence in Italian STPs, fate, and preliminary assessment on algal toxicity of amoxicillin.Environ. Sci. Technol. 38 (24), 6832-6838.

Andrews, J.M., 2001. Determination of minimum inhibitory concentrations. J. Antimicrob. Chemother. 48 (Suppl. 1), 5-16.

Ay, F., Kargi, F., 2011. Effects of reagent concentrations on advanced oxidation of amoxicillin by photo-Fenton treatment. J. Environ. Eng. 137 (6), 472-480.

Babington, R., Matas, S., Marco, M.P., Galve, R., 2012. Current bioanalytical methods for detection of penicillins. Anal. Bioanal. Chem. 403 (6), 1549-1566.

Barreiros, L., Nogales, B., Manaia, C.M., Ferreira, A.C.S., Pieper, D.H., Reis, M.A., Nunes, O.C., 2003. A novel pathway for mineralization of the thiocarbamate herbicide molinate by a defined bacterial mixed culture. Environ. Microbiol. 5 (10), 944-953.

Colina-Ma'rquez, J., MacHuca-Martı´nez, F., Puma, G.L., 2010. Radiation absorption and optimization of solar photocatalytic reactors for environmental applications. Environ. Sci. Technol. 44 (13), 5112-5120.

Daughton, C.G., Ternes, T.A., 1999. Pharmaceuticals and personal care products in the environment: agents of subtle change? Environ. Health Perspect. 107 (Suppl. 6), 907-938.

De Laat, J., Truong Le, G., Legube, B., 2004. A comparative study of the effects of chloride, sulfate and nitrate ions on the rates of decomposition of H2O2 and organic compounds by Fe(II)/H2O2 and Fe(III)/H2O2. Chemosphere 55 (5), 715-723.

236/98 Decreto-Lei n.o 236/98 de 1 de Agosto 1998, 1998. Dia'rio da Repu´ blica e I Se'rie-A, Portugal, pp. 3676-3722.

Deshpande, A.D., Baheti, K.G., Chatterjee, N.R., 2004. Degradation of beta-lactam antibiotics. Curr. Sci. 87 (12), 1684-1695.

Dimitrakopoulou, D., Rethemiotaki, I., Frontistis, Z., Xekoukoulotakis, N.P., Venieri, D., Mantzavinos, D., 2012. Degradation, mineralization and antibiotic inactivation of amoxicillin by UVeA/TiO2 photocatalysis. J. Environ. Manag. 98 (1), 168-174.

Drawz, S.M., Bonomo, R.A., 2010. Three decades of beta- lactamase inhibitors. Clin. Microbiol. Rev. 23 (1), 160-201.

Elmolla, E.S., Chaudhuri, M., 2011. Combined photo-FentoneSBR process for antibiotic wastewater treatment. J. Hazard. Mater. 192 (3), 1418-1426.

Faust, B.C., Zepp, R.G., 1993. Photochemistry of aqueous iron(III)-polycarboxylate complexes: roles in the chemistry of atmospheric and surface waters. Environ. Sci. Technol. 27 (12), 2517-2522.

Galleni, M., Lamotte-Brasseur, J., Rossolini, G.M., Spencer, J., Dideberg, O., Frere, J.M., 2001. Standard numbering scheme for class B beta-lactamases. Antimicrob. Agents Chemother. 45 (3), 660-663.

Gogate, P.R., Pandit, A.B., 2004a. A review of imperative technologies for wastewater treatment I: oxidation technologies at ambient conditions. Adv. Environ. Res. 8 (3-4), 501-551.

Gogate, P.R., Pandit, A.B., 2004b. A review of imperative technologies for wastewater treatment II: hybrid methods. Adv. Environ. Res. 8 (3-4), 553-597.

Gonzalez, L.J., Vila, A.J., 2012. Carbapenem resistance in Elizabethkingia meningoseptica is mediated by metallo-beta- lactamase BlaB. Antimicrob. Agents Chemother. 56 (4), 1686-1692.

Gonza'lez, O., Esplugas, M., Sans, C., Esplugas, S., 2008. Biodegradation of photo-fenton pre-treated solutions of sulfamethoxazole by aerobic communities. Molecular biology techniques applied to the determination of existing strains. J. Adv. Oxid. Technol. 11 (2), 238-245.

Gozlan, I., Rotstein, A., Avisar, D., 2013. Amoxicillin-degradation products formed under controlled environmental conditions: identification and determination in the aquatic environment. Chemosphere 91 (7), 985-992.

Guillard, C., Puzenat, E., Lachheb, H., Houas, A., Herrmann, J.M., 2005. Why inorganic salts decrease the TiO2 photocatalytic efficiency. Int. J. Photoenergy 7 (1), 1-9.

Henriques, I.S., Araujo, S., Azevedo, J.S., Alves, M.S., Chouchani, C., Pereira, A., Correia, A., 2012. Prevalence and diversity of carbapenem-resistant bacteria in untreated drinking water in Portugal. Microb. Drug Resist. 18 (5), 531-537.

Hirsch, R., Ternes, T., Haberer, K., Kratz, K.L., 1999. Occurrence of antibiotics in the aquatic environment. Sci. Total Environ. 225 (1-2), 109-118.

Homem, V., Alves, A., Santos, L., 2010. Amoxicillin degradation at ppb levels by Fenton's oxidation using design of experiments. Sci. Total Environ. 408 (24), 6272-6280.

Jeong, J., Yoon, J., 2005. pH effect on OH radical production in photo/ferrioxalate system. Water Res. 39 (13), 2893-2900.

Jerzsele, A., Nagy, G., 2009. The stability of amoxicillin trihydrate and potassium clavulanate combination in aqueous solutions. Acta Veterinaria Hung. 57 (4), 485-493.

Kim, O.S., Cho, Y.J., Lee, K., Yoon, S.H., Kim, M., Na, H., Park, S.C., Jeon, Y.S., Lee, J.H., Yi, H., Won, S., Chun, J., 2012. Introducing EzTaxon-e: a prokaryotic 16S rRNA gene sequence database with phylotypes that represent uncultured species. Int. J. Syst. Evol. Microbiol. 62 (Pt 3), 716-721.

Klamerth, N., Rizzo, L., Malato, S., Maldonado, M.I., Agu¨ era, A., Ferna'ndez-Alba, A.R., 2010. Degradation of fifteen emerging contaminants at mg L-1 initial concentrations by mild solar photo-Fenton in MWTP effluents. Water Res. 44 (2), 545-554.

Lamm, A., Gozlan, I., Rotstein, A., Avisar, D., 2009. Detection of amoxicillin-diketopiperazine-2', 5' in wastewater samples. J. Environ. Sci. Health Tox Hazard Subst. Environ. Eng. 44 (14), 1512-1517.

Lane, D.J., 1991. 16S/23S rRNA Sequencing. Wiley, New York. La€ngin, A., Alexy, R., Ko€nig, A., Ku¨ mmerer, K., 2009. Deactivation and transformation products in biodegradability testing of ß- lactams amoxicillin and piperacillin. Chemosphere 75 (3), 347-354.

Lewis, E.R., Winterberg, K.M., Fink, A.L., 1997. A point mutation leads to altered product specificity in beta-lactamase catalysis. Proc. Natl. Acad. Sci. U. S. A 94 (2), 443-447.

Li, G., Lv, L., Fan, H., Ma, J., Li, Y., Wan, Y., Zhao, X.S., 2010. Effect of the agglomeration of TiO2 nanoparticles on their photocatalytic performance in the aqueous phase. J. Colloid Interface Sci. 348 (2), 342-347.

Lindsey, M.E., Tarr, M.A., 2000. Inhibition of hydroxyl radical reaction with aromatics by dissolved natural organic matter. Environ. Sci. Technol. 34 (3), 444-449.

Literacka, E., Empel, J., Baraniak, A., Sadowy, E., Hryniewicz, W., Gniadkowski, M., 2004. Four variants of the Citrobacter freundii AmpC-Type cephalosporinases, including novel enzymes CMY-14 and CMY-15, in a Proteus mirabilis clone widespread in Poland. Antimicrob. Agents Chemother. 48 (11), 4136-4143.

Livermore, D.M., 1995. beta-Lactamases in laboratory and clinical resistance. Clin. Microbiol. Rev. 8 (4), 557-584.

Lopes, A.R., Danko, A.S., Manaia, C.M., Nunes, O.C., 2013. Molinate biodegradation in soils: natural attenuation versus bioaugmentation. Appl. Microbiol. Biotechnol. 97 (6), 2691-2700.

Malato, S., Ferna'ndez-Iba'n~ez, P., Maldonado, M.I., Blanco, J., Gernjak, W., 2009. Decontamination and disinfection of water by solar photocatalysis: recent overview and trends. Catal. Today 147 (1), 1-59.

Martinez, J.L., 2009. Environmental pollution by antibiotics and by antibiotic resistance determinants. Environ. Pollut. 157 (11), 2893-2902.

Mavronikola, C., Demetriou, M., Hapeshi, E., Partassides, D., Michael, C., Mantzavinos, D., Kassinos, D., 2009.

Mineralisation of the antibiotic amoxicillin in pure and surface waters by artificial UVA- and sunlight-induced fenton oxidation. J. Chem. Technol. Biotechnol. 84 (8), 1211-1217.

Michael, I., Rizzo, L., McArdell, C.S., Manaia, C.M., Merlin, C., Schwartz, T., Dagot, C., Fatta-Kassinos, D., 2013. Urban wastewater treatment plants as hotspots for the release of antibiotics in the environment: a review. Water Res. 47 (3), 957-995.

Na€gele, E., Moritz, R., 2005. Structure elucidation of degradation products of the antibiotic amoxicillin with ion trap MSn and accurate mass determination by ESI TOF. J. Am. Soc. Mass Spectrom. 16 (10), 1670-1676.

Nogueira, R.F.P., Oliveira, M.C., Paterlini, W.C., 2005. Simple and fast spectrophotometric determination of H2O2 in photo- Fenton reactions using metavanadate. Talanta 66 (1), 86-91.

Oller, I., Malato, S., Sa'nchez-Pe'rez, J.A., 2011. Combination of advanced oxidation processes and biological treatments for wastewater decontamination-a review. Sci. Total Environ. 409 (20), 4141-4166.

Panias, D., Taxiarchou, M., Douni, I., Paspaliaris, I., Kontopoulos, A., 1996. Thermodynamic analysis of the reactions of iron oxides: dissolution in oxalic acid. Can. Metall. Q. 35 (4), 363-373.

Pereira, J.H.O.S., Reis, A.C., Nunes, O.C., Borges, M.T., Vilar, V.J.P., Boaventura, R.A.R., 2013a. Assessment of solar driven TiO2- assisted photocatalysis efficiency on amoxicillin degradation. Environ. Sci. Pollut. Res., 1-12.

Pereira, J.H.O.S., Reis, A.C., Queiro's, D., Nunes, O.C., Borges, M.T., Vilar, V.P., Boaventura, R.A.R., 2013b. Insights into solar TiO2- assisted photocatalytic oxidation of two antibiotics employed in aquatic animal production, oxolinic acid and oxytetracycline. Sci. Total Environ. 463-464, 274-283.

Pereira, J.H.O.S., Queiro's, D.B., Reis, A.C., Nunes, O.C., Borges, M.T., Boaventura, R.A.R., Vilar, V.J.P., 2014. Process enhancement at near neutral pH of a homogeneous photo- Fenton reaction using ferricarboxylate complexes: application to oxytetracycline degradation. Chem. Eng. J. 253 (0), 217-228.

Pe'rez-Parada, A., Agu¨ era, A., Go'mez-Ramos, M.d.M., Garcı´a- Reyes, J.F., Heinzen, H., Ferna'ndez-Alba, A.R., 2011. Behavior of amoxicillin in wastewater and river water: identification of its main transformation products by liquid chromatography/ electrospray quadrupole time-of-flight mass spectrometry. Rapid Commun. Mass Spectrom. 25 (6), 731-742.

Pignatello, J.J., Oliveros, E., MacKay, A., 2006. Advanced oxidation processes for organic contaminant destruction based on the Fenton reaction and related chemistry. Crit. Rev. Environ. Sci. Technol. 36 (1), 1-84.

R Development Core Team, 2013. R: a Language and Environment for Statistical Computing. R Foundation for Statistical Computing, Vienna, Austria.

Reyns, T., Cherlet, M., De Baere, S., De Backer, P., Croubels, S., 2008. Rapid method for the quantification of amoxicillin and its major metabolites in pig tissues by liquid chromatography- tandem mass spectrometry with emphasis on stability issues. J. Chromatogr. B Anal. Technol. Biomed. Life Sci. 861 (1), 108-116.

Rizzo, L., Manaia, C., Merlin, C., Schwartz, T., Dagot, C., Ploy, M.C., Michael, I., Fatta-Kassinos, D., 2013. Urban wastewater treatment plants as hotspots for antibiotic resistant bacteria and genes spread into the environment: a review. Sci. Total Environ. 447, 345-360.

Rodrı´guez, S.M., Ga'lvez, J.B., Rubio, M.I.M., Iba'n~ez, P.F., Padilla, D.A., Pereira, M.C., Mendes, J.F., De Oliveira, J.C., 2004. Engineering of solar photocatalytic collectors. Sol. Energy 77 (5), 513-524.

Soares, P.A., Silva, T.F.C.V., Manenti, D.R., Souza, S.M.A.G.U., Boaventura, R.A.R., Vilar, V.J.P., 2014. Insights into real cotton- textile dyeing wastewater treatment using solar advanced oxidation processes. Environ. Sci. Pollut. Res. 21 (2), 932-945.

Sun, L., Klein, E.Y., Laxminarayan, R., 2012. Seasonality and temporal correlation between community antibiotic use and resistance in the United States. Clin. Infect. Dis. 55 (5), 687-694.

Torres, M.J., Ariza, A., Fernandez, J., Moreno, E., Laguna, J.J., Montanez, M.I., Ruiz-Sanchez, A.J., Blanca, M., 2010. Role of minor determinants of amoxicillin in the diagnosis of immediate allergic reactions to amoxicillin. Allergy 65 (5), 590-596.

Trovo', A.G., Pupo Nogueira, R.F., Agu¨ era, A., Fernandez-Alba, A.R., Malato, S., 2011. Degradation of the antibiotic amoxicillin by photo-Fenton process e chemical and toxicological assessment. Water Res. 45 (3), 1394-1402.

Vaz-Moreira, I., Nunes, O.C., Manaia, C.M., 2011. Diversity and antibiotic resistance patterns of Sphingomonadaceae isolates from drinking water. Appl. Environ. Microbiol. 77 (16), 5697-5706.

Vaz-Moreira, I., Nunes, O.C., Manaia, C.M., 2014. Bacterial diversity and antibiotic resistance in water habitats: searching the links with the human microbiome. FEMS Microbiol. Rev. 38 (4), 761-778.

Versporten, A., Coenen, S., Adriaenssens, N., Muller, A., Minalu, G., Faes, C., Vankerckhoven, V., Aerts, M., Hens, N., Molenberghs, G., Goossens, H., Metz, S., Fluch, G., Vaerenberg, S., Goossens, M.M., Markova, B., Andra sevic', A.T., Kontemeniotis, A., Vlc ek, J., Frimodt-Møller, N., Jensen, U.S., Rootslane, L., Laius, O., Vuopio-Varkila, J., Lyytikainen, O., Cavalie, P., Kern, W., Giamarellou, H., Antoniadou, A., Terna'k, G., Benko, R., Briem, H., Einarsson, O., Cunney, R., Oza, A., Raz, R., Edelstein, H., Folino, P., Seilis, A., Dumpis, U., Valinteliene, R., Bruch, M., Borg, M., Zarb, P., Natsch, S., Kwint, M., Blix, H.S., Hryniewics, W., Olczak-Pienkowska, A., Kravanja, M., Ozorowski, T., Ribeirinho, M., Caldeira, L., Băicus, , A., Popescu, G., Ratchina, S., Kozlov, R., Folta'n, V., C iz man, M., La'zaro, E., Campos, J., de Abajo, F., Dohnhammar, U., Zanetti, G., Davey, P., Wickens, H., 2011. European surveillance of antimicrobial consumption (ESAC): outpatient penicillin use in Europe (1997e2009). J. Antimicrob. Chemother. 66 (Suppl. 6), vi13-vi23.

Walsh, T.R., Toleman, M.A., Poirel, L., Nordmann, P., 2005. Metallo-beta-lactamases: the quiet before the storm? Clin. Microbiol. Rev. 18 (2), 306-325.

Zhang, Y., Marrs, C.F., Simon, C., Xi, C., 2009. Wastewater treatment contributes to selective increase of antibiotic resistance among Acinetobacter spp. Sci. Total Environ. 407 (12), 3702-3706.

Zhang, T., Shao, M.F., Ye, L., 2012. 454 pyrosequencing reveals bacterial diversity of activated sludge from 14 sewage treatment plants. ISME J. 6 (6), 1137-1147.

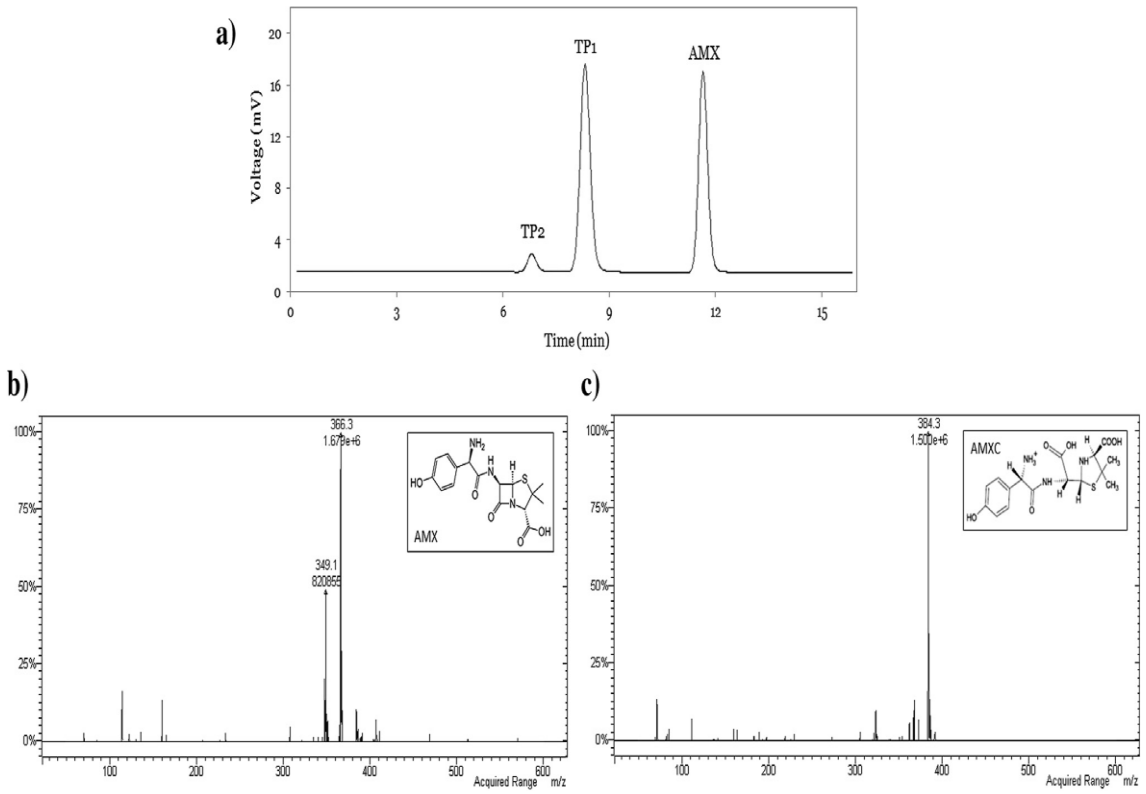

Fig. 1 - a) Chromatograms obtained by HPLC-UV/Vis analysis at 230 nm. Retention times of the compounds are: AMX: 12.1 min; TP1: 8.2 min and TP2: 6.9 min; b) MS/MS spectrum of Amoxicillin [m/z = 366]; c) MS/MS of Amoxicilloic acid [m/z = 384].

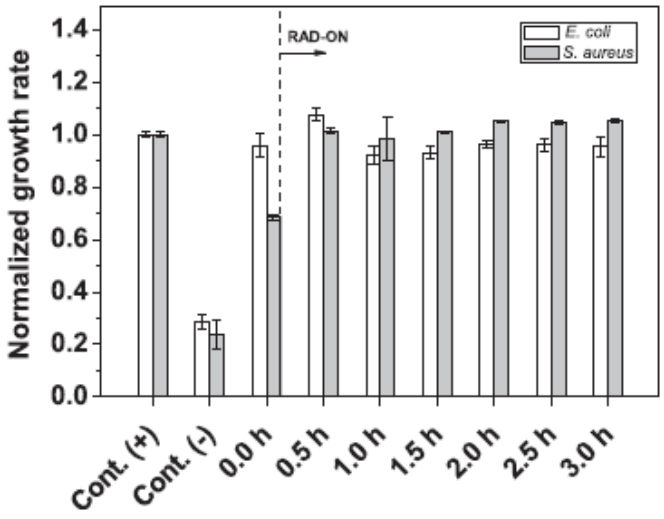

Fig. 2 - Normalized growth rate in samples taken in the Bio-photo-Fenton combined process in NaCl matrix, at pH_0 = 5.0. Values represent means and standard deviation (n = 3). Control (–) and Time 0.0 h are representative of the beginning and the end of the biological step. Time 0.5 h and onwards represent the photo-treatment period.

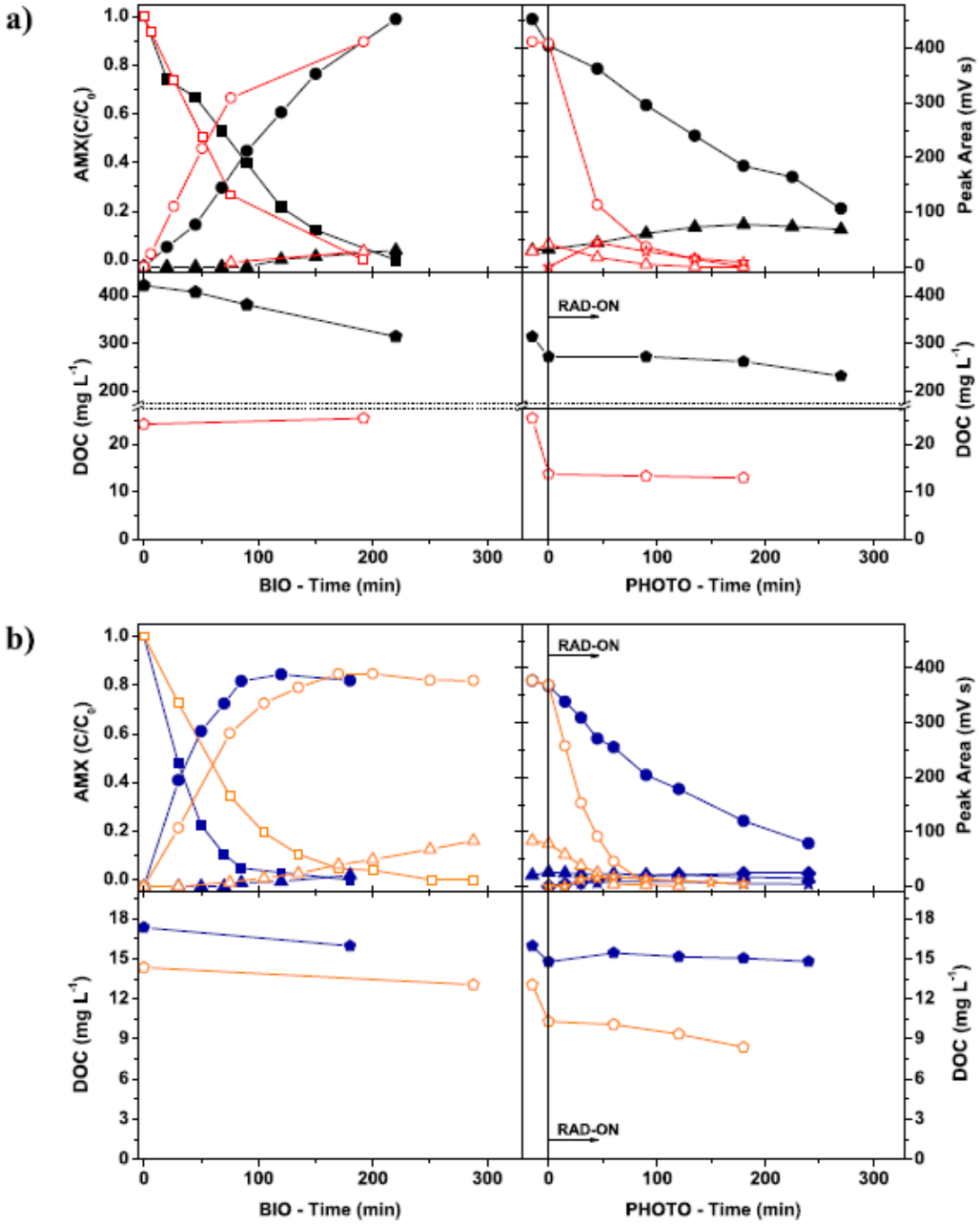

Fig. 3 - Follow-up of the Bio-TiO2 combined process on the degradation of AMX (square), its resulting transformation products (TP1 ∈ circle; TP2 ∈ triangle, TP3 ∈ star, TP4 ∈ diamond) and DOC (pentagon), using: a) EM (black symbols) or Buffer (red symbols); b) WW (blue symbols) or Cl (orange symbols). $[AMX]_0$ = 20 mg L^{-1}, Photocatalytic process parameters: $[TiO_2]$ = 0.2 g L^{-1}, pH_0 = 5.5, T = 25 ^{o}C, I = 44 W_{UV} m^{-2}. (For interpretation of the references to colour in this figure legend, the reader is referred to the web version of this article.)

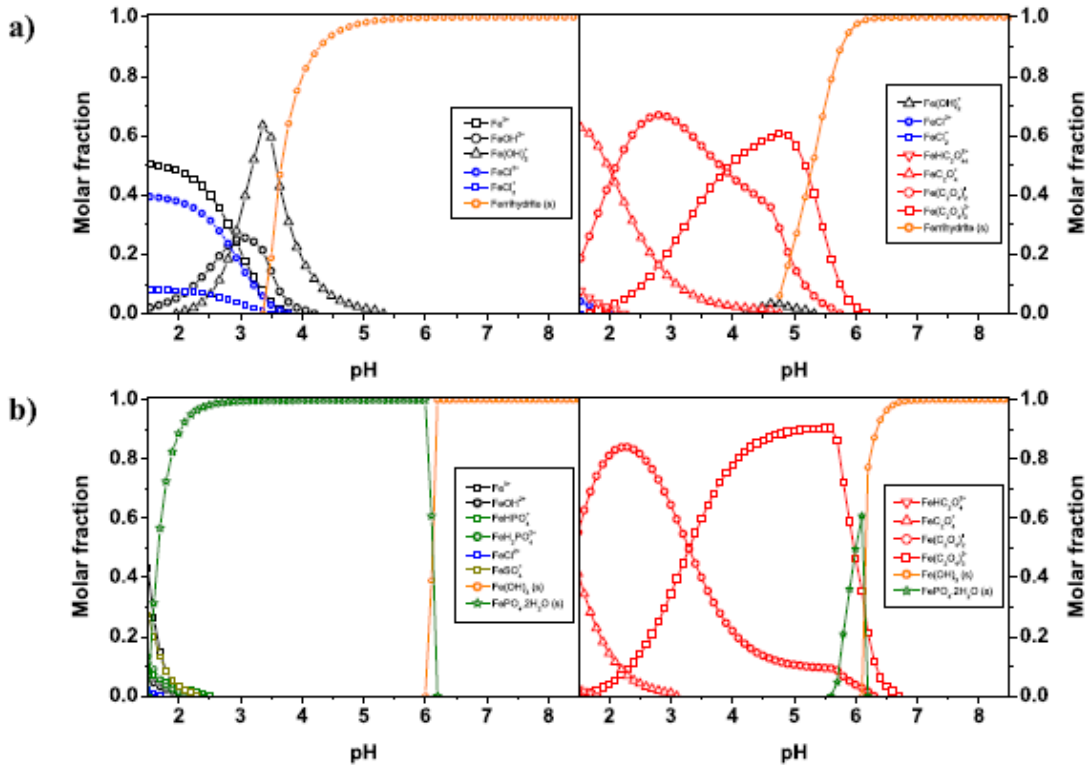

Fig. 4 - Speciation diagrams for iron(III) species as a function of pH in: a) NaCl matrix: without accounting (left) or accounting (right) for 1.07 × 10-^{1} mM (9.5 mg L^{-1}) oxalic acid; [Fe (III)] = 3.58 × 10^{-2} mM (2 mg L^{-1}), Ionic strength = 0.15 M; and b) WW matrix: without accounting (left) or accounting (right) for 3.22 × 10^{-1} mM (29 mg L^{-1}) oxalic acid. [Fe (III)] = 3.58 × 10^{-2} mM (2 mg L^{-1}). Ionic strength = 3.3 mM. The speciation software MINEQL+ was used to calculate the data.

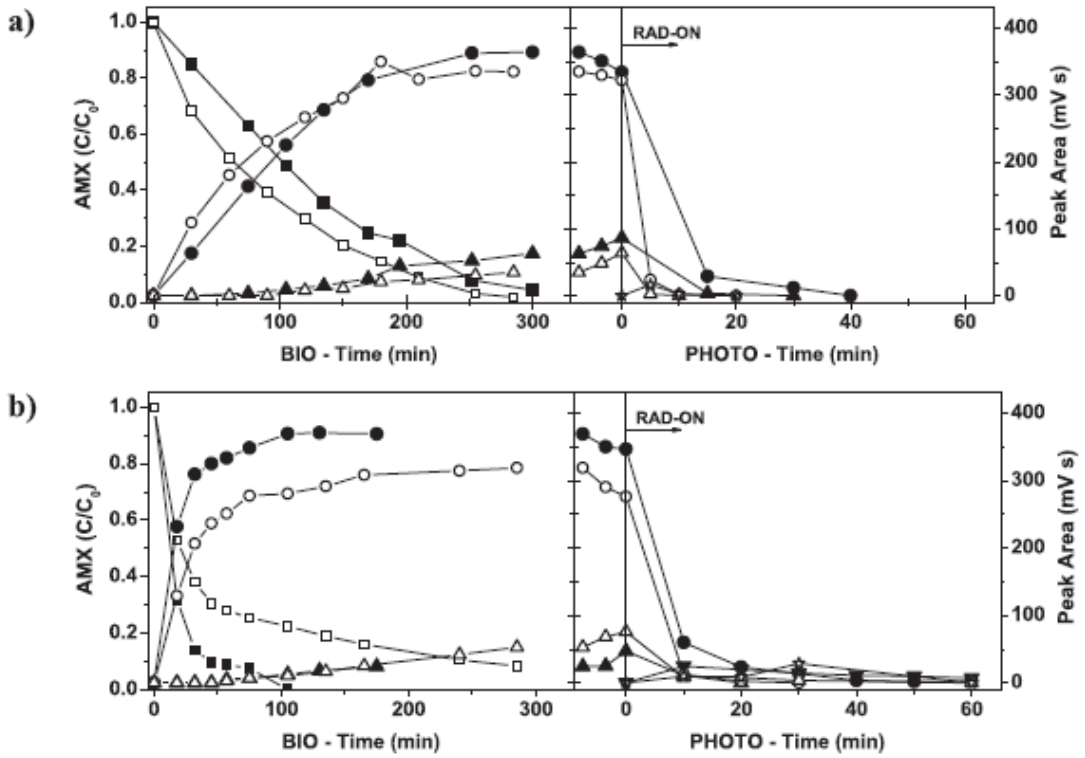

Fig. 5 - Evolution profiles of AMX (square) and its transformation products (TP1 - circle; TP2 - triangle, TP3 - star) during the Bio-Fe^{3+}/Oxalate/H_2O_2/UV-Vis combined process performed in a) NaCl matrix, and b) WW matrix. The pH in the photocatalytic step was adjusted to 4.0 (open symbols) or to 5.0 (closed symbols).

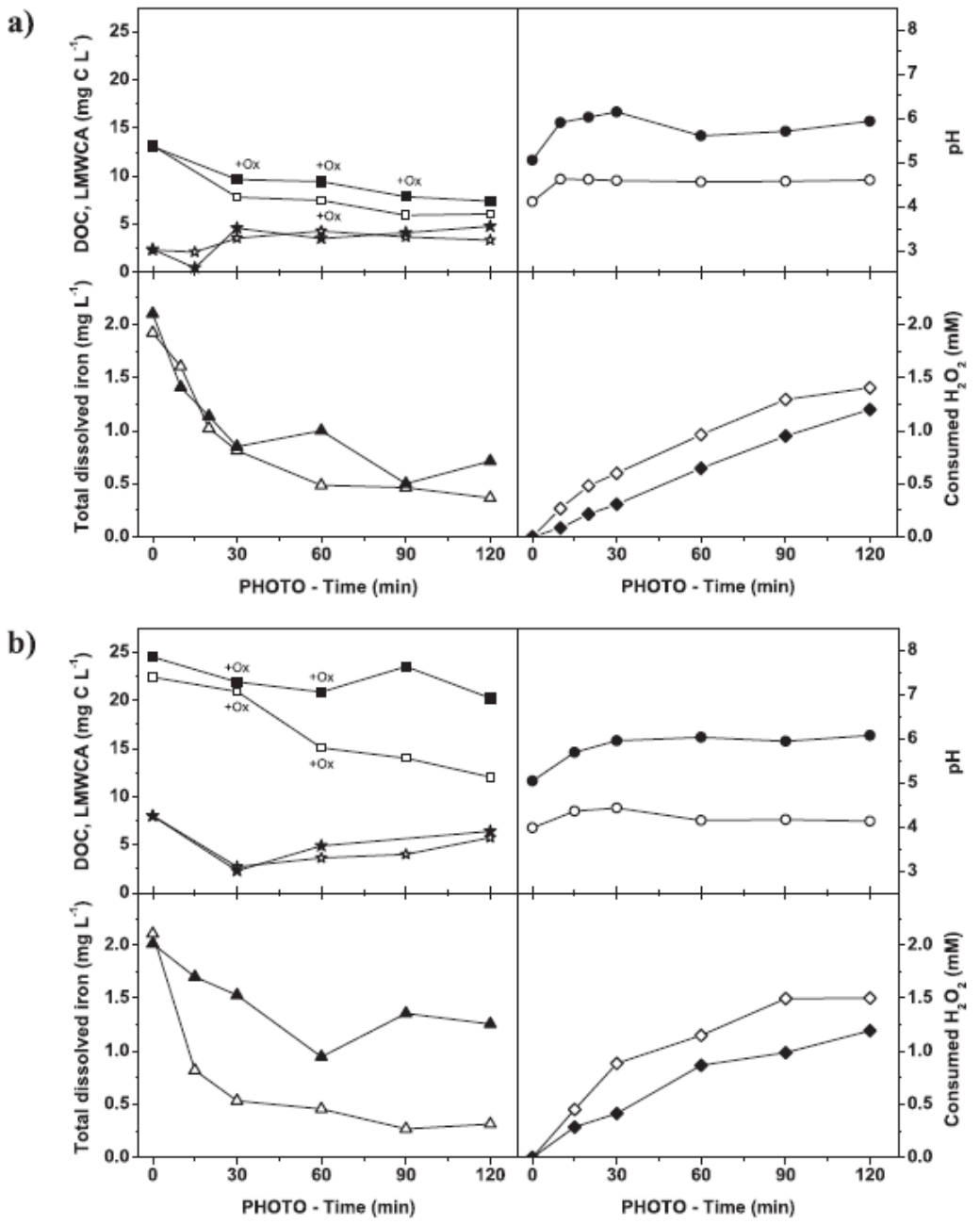

Fig. 6 - Follow-up of DOC removal (square), sum of LMWCA (star), pH (circle), total dissolved iron (triangle) and H2O2 consumption (diamond) during the photocatalytic stage of the Bio-Fe^{3+}/Oxalate/H2O2/UV-Vis combined process performed in: a) NaCl matrix, and b) WW matrix, at pH = 4.0 (open symbols) or pH = 5.0 (closed symbols). Process parameters: [Fe (III)] = 2 mg L^{-1}, initial 1:3 (NaCl) or 1:9 (WW) iron/oxalate molar ratio, total added H2O2 = 90 mg L^{-1}, T = 25 ^{o}C, I = 44 WUV m^{-2}. +Ox represents extra additions of oxalic acid.

Table 1 – Main characteristics of the used aqueous matrices before MC inoculation.

Matrix	pH	DOC/IC (mg L^{-1})	Ionic strength (M)	Average anion concentrations (g L^{-1})		
				$[PO_4^{3-}]$	$[Cl^-]$	$[SO_4^{2-}]$
EM	7.2	421/4.2	0.039	2.56	0.34	0.38
Buffer	7.2	Residual	0.050	4.75	<LOD	<LOD
NaCl	6.5	Residual	0.145	<LOD	5.15	<LOD
WW	6.8	5.6/4.9	0.003	0.01	0.06	0.04

LOD – Limit of detection.

Table 2 – Identification of bacterial strains recovered from the AMX-enriched culture (MC).

Phylum/Class	Species	Type strain	GenBank accession no.	No. of isolates	Length (bp)	16S rRNA gene sequence similarity (%)
Proteobacteria/Gammaproteobacteria	*Citrobacter freundii*	ATCC8090	ANAV01000046	13	860–1333	99.83–100
	Stenotrophomonas acidaminiphila	AMX19	AF273080	5	1219–1326	99.09–100
	Pseudomonas guariconensis	PCAVU11	HF674459	4	1273–1314	99.92
	Stenotrophomonas nitritireducens	L2	AJ012229	1	1372	99.93
Proteobacteria/Alphaproteobacteria	*Sphingomonas molluscorum*	KMM3882	AB248285	1	1290	99.84
Bacteroidetes/Sphingobacteriia	*Sphingobacterium multivorum*	IAM14316	AB100738	5	623–1268	99.21–100
Bacteroidetes/Flavobacteriia	*Elizabethkingia meningoseptica*	ATCC13253	ASAN01000081	4	770–1244	99.48–99.90

Table 3 – Zero-order kinetic parameters for AMX depletion by the MC in different aqueous matrices. $[AMX]_0 = 0.02\ g\ L^{-1}$; Incubation $T = 30\ °C$; Continuous shaking at 120 rpm; $V_0 = 1.2\ L$. All experiments were performed at near-neutral pH.

Matrix	Incubation time (h)	Biomass content ($mg\ L^{-1}$)	Specific degradation rate ($g_{AMX}\ g_{biomass}^{-1}\ h^{-1}$)	Half-life ($t_{1/2}$, h)
EM	3.7	26 ± 3	n.d.	n.d.
Buffer	3.2	112 ± 1	0.10 ± 0.01	0.9 ± 0.1
NaCl	4.8	(26 ± 1) × 10	0.03 ± 0.01	1.5 ± 0.3
WW	3.8	(21 ± 4) × 10	0.13 ± 0.07	0.5 ± 0.2

n.d. – not determined. Values represent means ± standard deviation.